Inorganic Chemistry
Article
pubs.acs.org/IC

Solvent Templates Induced Porous Metal–Organic Materials: Conformational Isomerism and Catalytic Activity

Ran Ding, Chao Huang, Jingjing Lu, Junning Wang, Chuanjun Song, Jie Wu,* Hongwei Hou,* and Yaoting Fan

College of Chemistry and Molecular Engineering, Zhengzhou University, Henan 450052, China

Ⓢ *Supporting Information*

ABSTRACT: Solvent templates induced Co-based metal–organic materials; conformational isomers $\{[Co_2(pdpa)(CH_3CN)(H_2O)_3]\cdot CH_3OH\cdot H_2O\}_n$ (**1**) and $\{[Co_2(pdpa)(CH_3CN)(H_2O)_3]\}_n$ (**2**) and $\{[Co_5(pdpa)_2(\mu_3\text{-}OH)_2(H_2O)_6]\cdot 2H_2O\}_n$ (**3**) [H_4pdpa = 5,5′-(pentane-1,2-diyl)-bis(oxy)diisophthalic acid] were synthesized under the same solvothermal conditions except with different concentrations of cyclic ethers (1,4-dioxane or tetrahydrofuran) as structure-directing agents. Structural transformations from a three-dimensional (3D) framework of **1** containing channels with dimensions of ∼6 Å × 6 Å to a two-dimensional layer structure of **2** consisting of large open channels with a size of ∼15 Å × 8 Å and then to a 3D nonporous framework of **3**, resulting from the different concentrations of cyclic ethers, were observed. The anion–π interactions between electron-efficient oxygen atoms of cyclic ethers and electron-deficient dicarboxylic acid aromatic cores in H_4pdpa imported into the synthetic process accounted for the conformational change of the ligand H_4pdpa and the following structural variations. A systematic investigation was conducted to explore how different concentrations of structure-directing agents affected the frameworks of resultant metal–organic frameworks. Furthermore, **1**–**3** were shown to be available heterogeneous catalysts for the synthesis of 2-imidazoline and 1,4,5,6-tetrahydropyrimidine derivatives by the cascade cycloaddition reactions of aromatic nitriles with diamines. The results showed that the catalytic activity of **2** was much higher than that of **1** and **3**, because of its unique structural features, including accessible catalytic sites and suitable channel size and shape. In addition, a plausible mechanism for these catalytic reactions was proposed, and the reactivity–structure relationship was further clarified.

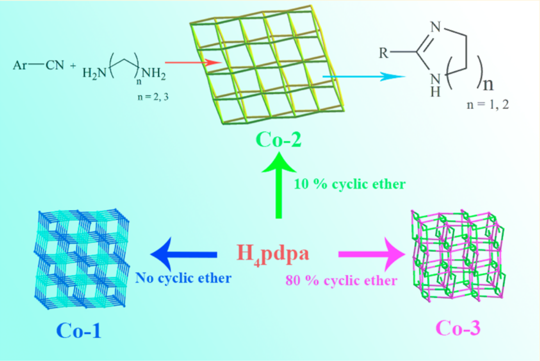

■ INTRODUCTION

The use of metal–organic frameworks (MOFs) as heterogeneous catalysts has attracted a growing amount of attention because they combine the advantages of both homogeneous and heterogeneous catalysts without their disadvantages.[1] For example, they are the building blocks of MOFs [i.e., metal centers at the nodes of the constituent secondary building units (SBUs) and organic linkers], and the supramolecular structures can be carefully tuned to adapt various catalytic reactions.[2] The ability to easily isolate, reuse, and recover MOF-based catalysts is also desirable for simplifying operation and reducing the levels of pollution and waste.[3] In addition, an important advantage of MOFs as heterogeneous catalysts is the fact that their porous frameworks permit substrates to be transported and to interact rapidly while possessing exceptional shape selectivity, size selectivity, chemoselectivity, and enantioselectivity.[4] These excellent features of MOF catalysts are mostly attributed to their flexible and diverse structures. Though it is still difficult to precisely predict the final structure of coordination assembly, researchers have summarized many factors that can influence the formation of MOFs, including the metal ion, organic ligand, reaction time, temperature, pressure, pH value, etc.[5] Furthermore, solvent as an external stimuli can also affect the coordination assemblies of specific reactants from both thermodynamic and kinetic perspectives, yielding diverse MOFs.[6] The solvent templates are not only shape-selective but also site-selective, resulting from their polarity,[7] bulkiness,[8] and interactions with metal sites or organic ligands of MOFs, such as a coordination bond,[9] a hydrogen bond,[10] an anion–π bond,[11] and an XH π-type bond (X = O, N, or C).[12] It has been determined that coordination assemblies are affected by solvent templates in two disparate ways: (i) solvent molecules as ligands and/or guests stay in the crystalline lattice to affect the product structure, and (ii) solvent molecules as structure-directing agents influence the crystal growth, framework, and final morphology yet do not exist in the final structure.[13] The structure-directing effect of solvents is more suitable for synthesizing heterogeneous MOF catalysts because solvent molecules located within channels will prevent the diffusion of reactants and products in the solid interior. Besides, removing the solvents will leave unsaturated coordination positions of

Received: September 29, 2014

DOI: 10.1021/ic502369y
Inorg. Chem. XXXX, XXX, XXX–XXX

catalytically active metal sites free to capture substrates. Though a few examples of coordination assemblies affected by the structure-directing effect of solvent molecules have been reported and have become some of the most fascinating phenomena in crystallography and materials science,[14] the intricate mechanism involved in these solvent-directed coordination assemblies remains largely unclear.

Especially, in some cases, solvent templates as structure-directing agents do not change the SBUs or chemical compositions of resultant MOFs but simply change the conformation of their structural skeletons, resulting in the formation of conformational isomers (also called as polymorphs).[15] Conformational isomers of MOFs have attracted a great deal of interest in the field of heterogeneous catalysis in recent years because the isomers have identical SBUs and organic ligands, providing a useful platform for exploring the role of the structural features of MOFs in their shape and size selectivity during catalytic reactions.[16] In previous reports, it has been summarized that the conformational isomers could be obtained by altering the solvent system from polar to nonpolar,[7] organic to inorganic,[17] or dry to wet.[18] However, examples of solvent-induced conformational isomers remain rare.[14]

Herein, we present a series of Co-based MOFs, conformational isomers $\{[Co_2(pdpa)(CH_3CN)(H_2O)_3]\cdot CH_3OH\cdot H_2O\}_n$ (**1**) and $\{[Co_2(pdpa)(CH_3CN)(H_2O)_3]\}_n$ (**2**) and $\{[Co_5(pdpa)_2(\mu_3\text{-}OH)_2(H_2O)_6]\cdot 2H_2O\}_n$ (**3**) [H_4pdpa = 5,5′-(pentane-1,2-diyl)-bis(oxy)diisophthalic acid], which were synthesized under the same sovlothermal conditions except with different concentrations of cyclic ethers [1,4-dioxane or tetrahydrofuran (THF)] as structure-directing agents. With the concentration of solvent-directing agents increasing, the resultant structures transformed from a three-dimensional (3D) porous framework of **1** to a two-dimensional (2D) porous structure of **2** and then to a 3D nonporous **3**. In particular, **1** and **2** are solvent-induced conformational isomers. We reasoned that the structural variations among **1**−**3** result from the conformational transformation of ligand H_4pdpa caused by the anion−π interaction between cyclic ethers and ligand H_4pdpa.[11] In addition, we demonstrated the catalytic potential of **1**−**3** with respect to the synthesis of 2-imidazoline and 1,4,5,6-tetrahydropyrimidine derivatives by the cascade cycloaddition reactions of diamines with aromatic nitriles. The structure−activity relationship was clarified, indicating the important roles of channel size and coordination environment of metal sites in these catalytic reactions.

■ EXPERIMENTAL SECTION

Materials and Physical Measurements. All reagents and solvents were commercially available and used as received without further purification. H_4pdpa was synthesized according to a modified procedure from the literature.[19] The atomic absorption spectrum was recorded on a Z28000 graphite-oven atomic absorption spectrophotometer. Fourier transform infrared spectra were recorded on a Bruker-ALPHA spectrophotometer with KBr pellets in the 400−4000 cm^{-1} region. Elemental analyses (C, H, and N) were conducted on a FLASH EA 1112 elemental analyzer. Powder X-ray diffraction (PXRD) patterns were recorded using Cu Kα_1 radiation on a PANalyticalX'Pert PRO diffractometer. Thermogravimetric analyses (TGA) were performed on a Netzsch STA 449C thermal analyzer at a heating rate of 10 °C min^{-1} in air. ^{1}H and ^{13}C nuclear magnetic resonance (NMR) spectra were recorded with Bruker Avance-300 spectrometers. Liquid chromatography−mass spectrometry spectra were measured on an Agilent MSD-1100 ESI-MS/MS system. The pore size distributions of **2** were collected on a Micromeritics ASAP 2420 Accelerated Surface Area and Porosimetry System under ultrahigh vacuum in a clean system, with a diaphragm and turbo pumping system. Ultra-high-purity-grade (>99.999%) N_2 gas was used in all adsorption measurements. The experimental temperature was maintained with liquid nitrogen (77 K). Prior to measurement, the bulk sample of **2** was washed with absolute ethanol (EtOH) three times, dried under vacuum, and then transferred into a stainless steel column. After 20 min of soaking and venting of supercritical CO_2 (SC-CO_2) by a DB-80 simplex pump, the column pressure regulator was set at 109 bar by soaking SC-CO_2 and the column temperature was increased to 60 °C. SC-CO_2 in the column was gradually vented after 12 h.

Synthesis of $\{[Co_2(pdpa)(CH_3CN)(H_2O)_3]\cdot CH_3OH\cdot H_2O\}_n$ (1). A mixture of $Co(NO_3)_2\cdot 6H_2O$ (0.058 g, 0.2 mmol), H_4pdpa (0.043 g, 0.1 mmol), NaOH (0.016 g, 0.4 mmol), and a 1:2:8 $CH_3CN/CH_3OH/H_2O$ mixture (10 mL) was placed in a 25 mL Teflon-lined stainless steel container. The container was sealed and heated at 160 °C for 3 days. After the mixture had cooled to ambient temperature at a rate of 5 °C/h, purple crystals of **1** were obtained with a yield of 34% (based on Co). Anal. Calcd for $C_{24}H_{31}Co_2NO_{15}$: C, 41.69%; H, 4.52%; N, 2.03%. Found: C, 41.58%; H, 4.69%; N, 2.17%. IR (KBr, cm^{-1}): 3343 (m), 3072 (w), 2268 (s), 1616 (m), 1453 (w), 1264 (m), 1043 (s), 773 (s), 713 (w).

Synthesis of $\{[Co_2(pdpa)(CH_3CN)(H_2O)_3]\}_n$ (2). A mixture of $Co(NO_3)_2\cdot 6H_2O$ (0.058 g, 0.2 mmol), H_4pdpa (0.043 g, 0.1 mmol), NaOH (0.016 g, 0.4 mmol), 1,4-dioxane (or THF) (1 mL), and a 1:2:8 $CH_3CN/CH_3OH/H_2O$ mixture (9 mL) was placed in a 25 mL Teflon-lined stainless steel container. The container was sealed and heated at 160 °C for 3 days. After the mixture had cooled to ambient temperature at a rate of 5 °C/h, purple crystals of **2** were obtained with a yield of 79% (based on Co). Anal. Calcd for $C_{23}H_{25}Co_2NO_{13}$: C, 43.08%; H, 3.93%; N, 2.18%. Found: C, 43.24%; H, 3.80%; N, 2.27%. IR (KBr, cm^{-1}): 3343 (m), 2946 (w), 2268 (s), 1616 (m), 1454 (w), 1266 (m), 1041 (s), 774 (s), 717 (w).

Synthesis of $\{[Co_5(pdpa)_2(\mu_3\text{-}OH)_2(H_2O)_6]\cdot 2H_2O\}_n$ (3). A mixture of $Co(NO_3)_2\cdot 6H_2O$ (0.058 g, 0.2 mmol), H_4pdpa (0.043 g, 0.1 mmol), NaOH (0.016 g, 0.4 mmol), a 1:2:8 $CH_3CN/CH_3OH/H_2O$ mixture (2 mL), and 1,4-dioxane (or THF) (8 mL) was placed in a 25 mL Teflon-lined stainless steel container. The container was sealed and heated at 160 °C for 3 days. After the mixture had cooled to ambient temperature at a rate of 5 °C/h, purple crystals of **3** were obtained with a yield of 65% (based on Co). Anal. Calcd for $C_{42}H_{50}Co_5O_{30}$: C, 37.94%; H, 3.79%. Found: C, 37.84%; H, 3.68%. IR (KBr, cm^{-1}): 3375 (m), 3149 (m), 1662 (m), 1506 (m), 1285 (w), 1007 (m), 745 (vw).

Typical Procedure for the Synthesis of 2-Imidazoline (7a−d) and 1,4,5,6-Tetrahydropyrimidine Derivatives (8a−d) with Catalysts 1−3. Nitrile (1.0 mmol, 1.0 equiv, **4a**−**d**), ethylenediamine or 1,3-diaminopropane (0.5 mL, **5** or **6**, respectively), catalyst (0.1 mmol, 0.1 equiv based on cobalt ions, **1**−**3**), and toluene (5 mL) were mixed and heated to reflux. After 4 h, the bulk of the cool solvent was filtered and evaporated in vacuo, and then the residue was partitioned between chloroform (25 mL) and H_2O (25 mL). The organic phase was washed with saturated aqueous NaCl, dried with Na_2SO_4, filtered, and evaporated in vacuo. The residue was purified by column chromatography on silica gel (3:1 EtOAc/MeOH). ^{1}H NMR spectra were recorded on a 300 MHz instrument and ^{13}C NMR spectra on a 75 MHz instrument.

Crystal Data Collection and Refinement. The data of **1**−**3** were collected on a Rigaku Saturn 724 CCD diffractometer (Mo Kα; λ = 0.71073 Å) at 20 ± 1 °C. Absorption corrections were applied by using a numerical program. The data were corrected for Lorentz and polarization effects. The structures were determined by direct methods and refined with a full-matrix least-squares technique based on F^2 with the SHELXL-97 crystallographic software package.[20] Hydrogen atoms were placed at calculated positions and refined as riding atoms with isotropic displacement parameters. The SQUEEZE program implemented in PLATON was used to remove electron densities in **2** and **3**, and the numbers of guest molecules for **2** and **3** were calculated by

TGA and elemental analysis data. Crystallographic crystal data and structure processing parameters for **1−3** are listed in Table 1. Selected bond lengths and bond angles for **1−3** are listed in Table S1 of the Supporting Information.

Table 1. Crystallographic Data and Refinement Parameters for 1−3

	1	2	3
formula	$C_{24}H_{31}O_{15}Co_2$	$C_{23}H_{25}O_{13}Co_2$	$C_{42}H_{50}O_{30}Co_5$
fw	691.36	641.30	1329.47
temp (K)	293(2)	293(2)	293(2)
wavelength (Å)	0.71073	0.71073	0.71073
crystal system	monoclinic	triclinic	orthorhombic
space group	$P2_1/c$	$P\bar{1}$	$Fdd2$
a (Å)	7.7720(16)	10.570(2)	23.362(5)
b (Å)	18.629(4)	10.659(2)	22.491(5)
c (Å)	19.518(5)	13.810(3)	22.738(5)
α (deg)	90	104.32(3)	90
β (deg)	104.23(3)	103.67(3)	90
γ (deg)	90	109.51(3)	90
V (Å^3)	2739.2(11)	1331.5(5)	11948(4)
Z	4	2	8
D_c (g cm^{-3})	1.676	1.600	1.478
μ (mm^{-1})	1.288	1.313	1.442
$F(000)$	1424	656	5416
GOF on F^2	1.133	0.959	0.953
no. of reflections collected	24436	6252	5531
no. of unique reflections	6487	6252	5531
R_1, wR_2 [$I > 2\sigma(I)$]^a	0.0720, 0.1932	0.0563, 0.1505	0.0869, 0.2160

$^a R_1 = \sum||F_o| - |F_c||/\sum|F_o|$. $wR_2 = [\sum w(F_o^2 - F_c^2)^2/\sum w(F_o^2)^2]^{1/2}$.

RESULTS AND DISCUSSION

Structure of $\{[Co_2(pdpa)(CH_3CN)(H_2O)_3]\cdot CH_3OH\cdot H_2O\}_n$ (1). X-ray analysis revealed that **1** is a 3D framework and crystallizes in the monoclinic crystal system $P2_1/c$. The asymmetric unit of **1** consists of two crystallographically independent Co(II) ions, one completely deprotonated pdpa^{4-} ligand, three coordinated water molecules, and one coordinated acetonitrile molecule (Figure S1 of the Supporting Information). Two Co(II) centers are connected by two carboxylate groups of pdpa^{4-} ligands to form a dinuclear $\{Co_2(CO_2)_2\}$ SBU. As shown in Figure 1a, the $\{Co_2(CO_2)_2\}$ SBUs are further extended by pdpa^{4-} ligands to construct infinite 2_1 helical motifs in *P*- and *M*-helicity, which should originate from the dihedral angle between the two aromatic rings of the pdpa^{4-} ligand being 20.0° and the distinct conformations of pdpa^{4-} ligand with two dicarboxylic acid aromatic cores pointing in different directions. A significant structural feature of **1** is that the helical spirals form open channel dimensions of ~6 Å × 6 Å (considering van der Waals radii) along the *a* axis. The helical channels are arranged alternatively in *P*- and *M*-helicity, leading to a 3D network with a mesomeric lattice (Figure 1b). Topologically, **1** can be considered as a 4,4-connected net with a topological point symbol of $\{4^2.8^4\}$ (Figure 1c).

Structure of $\{[Co_2(pdpa)(CH_3CN)(H_2O)_3]\}_n$ (2). **2** was successfully obtained under the same solvothermal conditions that were used for **1** except with the addition of 1,4-dioxane as a structure-directing agent (1:9 $V_{template}$:$V_{prior\ solvents}$). X-ray analysis indicated that **2** crystallizes in the triclinic crystal system $P\bar{1}$. The asymmetric unit of **2** consists of two independent Co(II) ions, one completely deprotonated pdpa^{4-} ligand, three coordinated water molecules, and one coordinated acetonitrile molecule (Figure S2 of the Supporting Information). As seen with **1**, four oxygen atoms from two carboxylate groups and two independent Co(II) ions construct a $\{Co_2(CO_2)_2\}$ SBU, which is approximately identical to that of **1**. Thus, **2** can be regarded as a conformational isomer of **1**. However, under the effect of solvent templates, the dihedral angle between two aromatic rings of a pdpa^{4-} ligand changes from 20.0° to 0.3°, which indicates that the conformation of the ligand transforms from distortion of **1** to planarity of **2**. Thus, two $\{Co_2(CO_2)_2\}$ SBUs and two pdpa^{4-} ligands form a closed circle instead of the helical spiral of **1**. All circles in the same plane are connected by pdpa^{4-} ligands or Co(II) SBUs, creating a 2D framework (Figure 2a). As shown in Figure 2b, these 2D sheets are stacked by $\pi\cdots\pi$ interactions with a distance of approximately 3.7 Å, creating a 3D layer framework including one-dimensional channels of ~15 Å × 8 Å (Figure 2b, considering van der Waals radii).

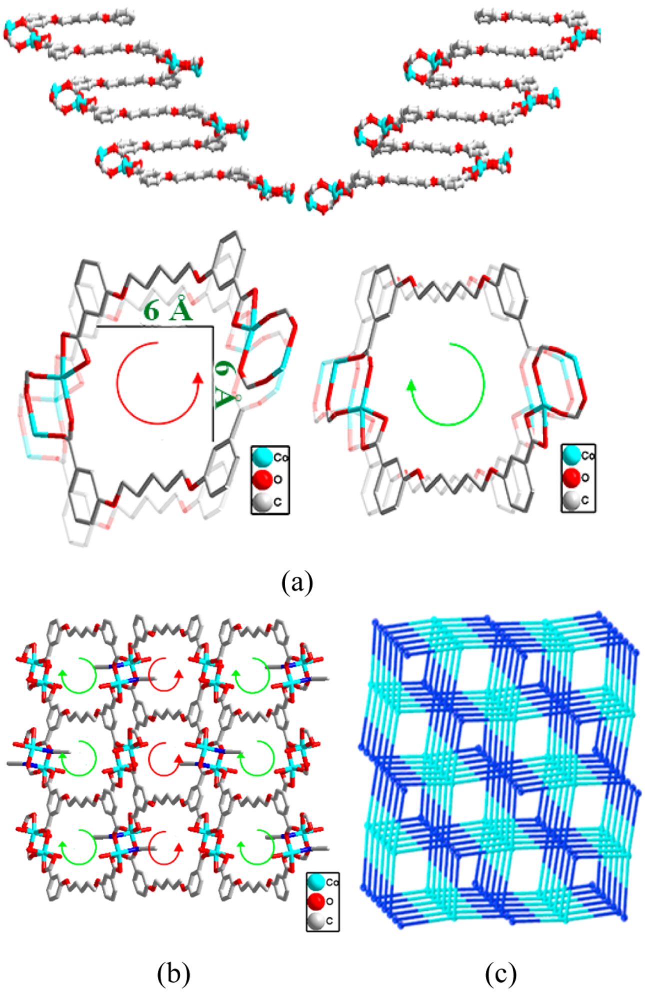

Figure 1. (a) View of the infinite 2_1 spiral chain along the *b* axis (top) and *a* axis (bottom). Red and green curved arrows indicate *P*- and *M*-helicity, respectively. (b) View of the 3D framework with helical spirals of **1**. (c) View of the 3D 4,4-connected net with a topological point symbol of $\{4^2.8^4\}$.

Structure of $\{[Co_5(pdpa)_2(\mu_3\text{-}OH)_2(H_2O)_6]\cdot 2H_2O\}_n$ (3). **3** was obtained under the conditions used for **2** except that the level of 1,4-dioxane was ≥80% (by volume) of the solvent

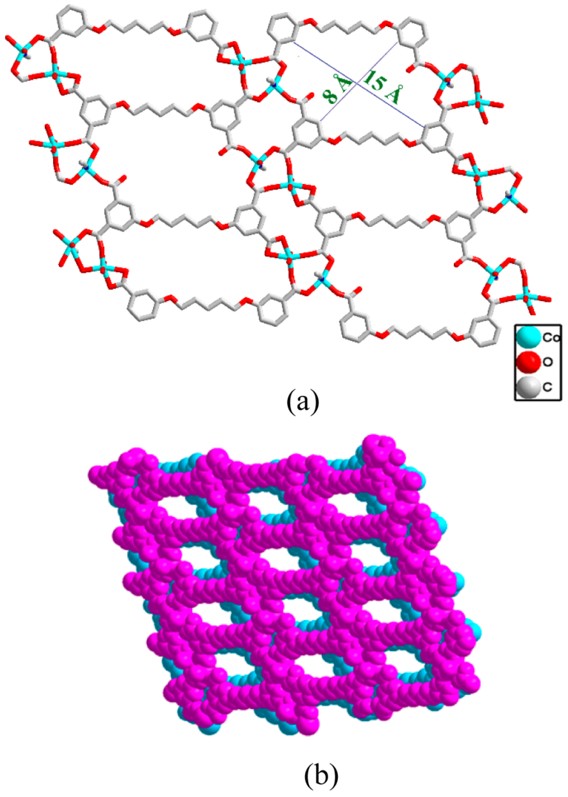

(a)

(b)

Figure 2. (a) View of the 2D network along the *b* axis. (b) Space-filling model of the 2D stacked layer framework containing one-dimensional channels.

mixture. The result of the crystallographic analysis revealed that **3** exhibits a compact 3D framework and crystallizes in the orthorhombic crystal system *Fdd*2. The asymmetric unit of **3** contains two and one-half Co(II) ions, one completely deprotonated pdpa^{4-} ligand, one μ_3-hydroxyl oxygen atom, and three coordinated water molecules (Figure S3 of the Supporting Information).

Five symmetry-related Co(II) atoms (Co1, Co2, Co3, Co2A, and Co3A) are linked together by two μ_3-hydroxyl oxygen atoms and two water molecules to construct a $[Co_5(\mu_3\text{-}OH)_2(H_2O)_2]$ cluster as a pentanuclear Co(II) SBU, which is completely different from the $\{Co_2(CO_2)_2\}$ SBU in **1** and **2**. Moreover, all carboxylate groups of symmetrical pdpa^{4-} ligands are deprotonated and adopt bismonodentate and monodentate coordination modes to bridge pentanuclear Co(II) SBUs, forming a 3D framework (Figure 3a). The pentanuclear Co(II) SBU can be defined as a unimodal 8-connected node, and the pdpa^{4-} ligand acts as 4-connected linkers. From a topological point of view, **3** can be considered to be a 4,8-connected net with a topological point symbol of $\{4^3.6^{23}.8^2\}\{4^3.6^3\}_2$ (Figure 3b).

Structure-Directing Effect of Solvent Templates. It has been demonstrated that solvent molecules as structure-directing agents can modulate the structures of MOFs, but the achievement still remains a scarcely explored field of research, especially for the synthesis of conformational isomers.[7]

Initially, **1** was obtained as the only product by heating a mixture of $Co(NO_3)_2\cdot6H_2O$ and Na_4pdpa in a 1:2:8 $CH_3CN/CH_3OH/H_2O$ mixture at 160 °C for 3 days and cooling it to ambient temperature at 5 °C/h. Interestingly, when we treated the reaction mixture under exactly the same conditions that are mentioned above except with the addition of a low concentration of 1,4-dioxane as a template (1:9 $V_{template}$:$V_{prior\ solvents}$), **2** was obtained as the only product. Therefore, the addition of a low concentration of 1,4-dioxane resulted in the 3D framework of **1** changing to 2D layer structure of **2**, in which the $\{Co_2(CO_2)_2\}$ SBUs remained invariable but the conformation of the pdpa^{4-} ligand transformed from slight distortion (20.0°) to planarity (0.3°). As a result, the channel size grows from ~6 Å × 6 Å for **1** to ~15 Å × 8 Å for **2**. By contrast, when the solvent volume ratio of 1,4-dioxane to prior solvents was increased to 4:1, **3** was obtained and exhibited a compact 3D framework with pentanuclear cobalt $[Co_5(\mu_3\text{-}OH)_2(H_2O)_2]$ SBUs, which were greatly different from the SBUs of **1** and **2**. The conformation of the pdpa^{4-} ligand returns to the distorted form (82.8°), and the coordination environment of metal sites is dense, suppressing the existence of available channels (Figure 4). Thus, a series of Co-based MOFs (**1**−**3**) were successfully obtained under the same solvothermal conditions except with different concentrations of 1,4-dioxane as the structure-directing agent.

The fact that the same reactions conducted at different concentrations of 1,4-dioxane afforded entirely different frameworks prompted us to take a systematic approach to

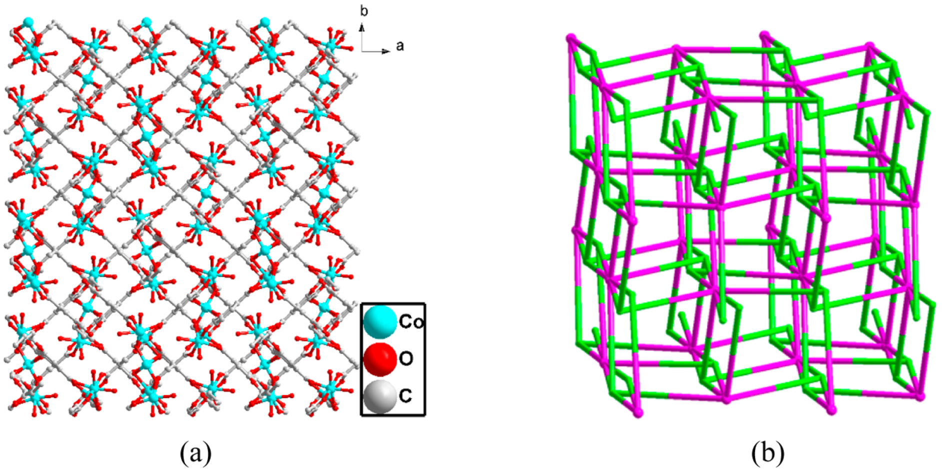

(a) (b)

Figure 3. (a) View of the compact 3D stacked plot of **3** along the *c* axis. (b) View of the 3D 4,8-connected net with a topological point symbol of $\{4^3.6^{23}.8^2\}\{4^3.6^3\}_2$.

DOI: 10.1021/ic502369y
Inorg. Chem. XXXX, XXX, XXX−XXX

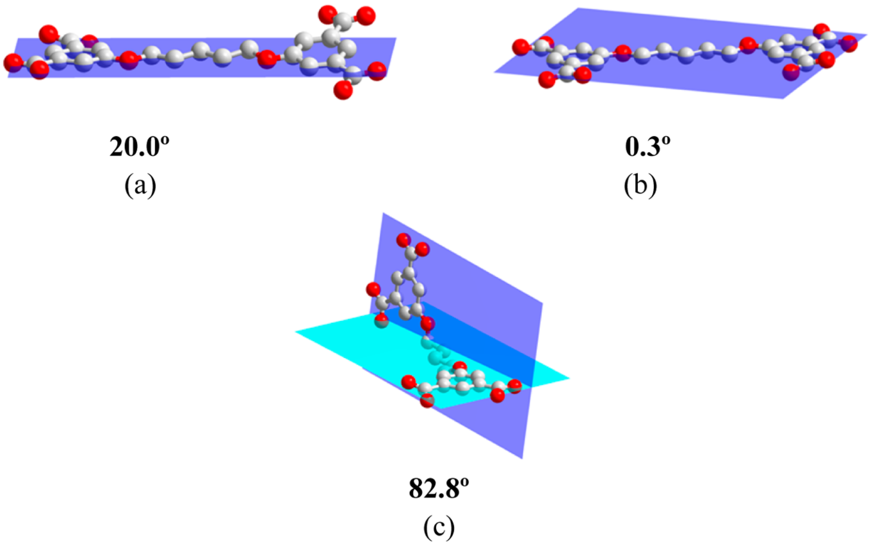

20.0°
(a)

0.3°
(b)

82.8°
(c)

Figure 4. View of the conformational variations of the H_4pdpa ligand among **1**−**3**: (a) slight distortion in **1**, (b) planarity in **2**, and (c) distortion in **3**.

exploring what influence the concentration of structure-directing agents might have upon the framework of MOFs. The following observations are detailed in Table 2 and supported by PXRD patterns (Figure 5). (1) Without a solvent template, only **1** could be obtained. (2) The addition of a low concentration of template (1:9 < $V_{template}$:$V_{prior\ solvents}$ < 1:1) afforded **2**, whereas a high concentration of solvent template ($V_{template}$:$V_{prior\ solvents}$ > 4:1) led to **3**. (3) A mixture of **2** and **3** was obtained at an intermediate concentration of solvent template. The results indicated that the solvent volume ratio controlled the complexes' syntheses and a high concentration of solvent templates tended to favor **3** over **2**. We reasoned that the prior mixture of solvents H_2O, CH_3OH, and CH_3CN with a volume ratio of 8:2:1 favors the formation of dinuclear $\{Co_2(CO_2)_2\}$ units, which are the SBUs in both **1** and **2**. 1,4-Dioxane as structure-directing agent at low concentrations affects only the configuration of the ligand and has no influence on the $\{Co_2(CO_2)_2\}$ SBUs. In **1** and **2**, two aromatic rings of the ligand point in different directions, leading to the conformational isomerism. By contrast, with the 1,4-dioxane:prior solvent volume ratio increasing to more than half of the mixed solvents, **3** with $[Co_5(\mu_3\text{-OH})_2(H_2O)_2]$ SBUs begins to be generated, along with the formation of **2** with $\{Co_2(CO_2)_2\}$ SBUs. When the 1,4-dioxane:prior solvent volume ratio increases to >4:1, which favors the formation of the $[Co_5(\mu_3\text{-OH})_2(H_2O)_2]$ units instead of the $\{Co_2(CO_2)_2\}$ units, **3** is obtained as the only product.

Table 2. Summary of the Products Isolated at Different Proportions of Template Guest (1,4-dioxane or THF)

entry	volume ratio between template and prior solvent[a]	obtained product
1	none	**1**
2	1:9	**2**
3	2:8	**2**
4	3:7	**2**
5	4:6	**2**
6	5:5	**2**
7	6:4	**2** and **3**
8	7:3	**2** and **3**
9	8:2	**3**
10	9:1	**3**

[a] The prior solvent is a mixture of H_2O, CH_3OH, and CH_3CN with a volume ratio of 8:2:1.

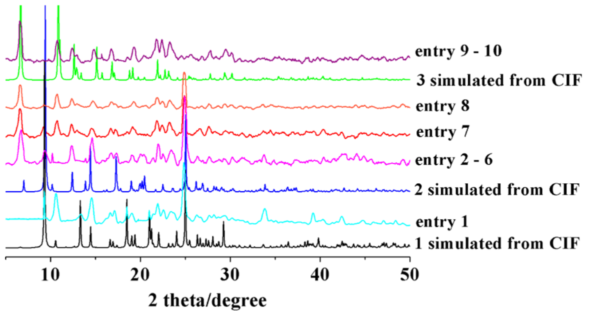

Figure 5. PXRD patterns for **1** simulated from a CIF file (black), **2** simulated from a CIF file (dark blue), **3** simulated from a CIF file (green), samples in entry 1 of Table 2 (cyan), samples in entries 2−6 of Table 2 (magenta), samples in entry 7 of Table 2 (red), samples in entry 8 of Table 2 (orange), and samples in entries 9 and 10 of Table 2 (violet).

Interestingly, THF, of which the polarity (dipole moment of 1.75) is much larger than that of 1,4-dioxane (dipole moment of 0.45),[21] could also be used as a structure-directing agent to obtain **2** and **3** with the same volume ratio of templates to prior solvents as 1,4-dioxane. It indicated that the solvent structure-directing effect herein did not result from the polarity. We attributed this solvent effect to the anion−π interactions between the electronegative oxygen atoms of cyclic ethers (1,4-dioxane or THF) and electron-deficient dicarboxylic acid aromatic cores in H_4pdpa because the electron-deficient π systems could operate as receptors capable of binding an anion or molecule with electronegative atoms.[11] Additionally, the addition of heterocyclic aromatic compounds (pyrrole, pyrazine, or imidazole) containing electronegative N atoms instead of cyclic ether (1,4-dioxane or THF) as a template at a low concentration (0.5 equiv) under the same reaction conditions also could achieve the structural transformation from **1** to **2**. In comparison, adding solvents such as chloroform, dichloromethane, cyclohexane, dimethylformamide (DMF), morpholine, and *N*-methyl-2-pyrrolidone (NMP) could not produce **1**−**3** successfully. The results further validated our inference that the anion−*π* interactions of templates and ligands accounted for the conformational change of ligand H_4pdpa and the following structural variations.

Though it has been well demonstrated that the coordination assemblies of specific reactants will be affected by the solvents used in reactions to influence the crystal growth, crystalline morphology, and lattice structure of the final solid, studies that aimed to determine if the ratio of template to a mixed solvent is a controlling factor in determining the ultimate topologies of a series of MOFs are really rare.[22] Besides, we proved that the templates in this work as structure-directing agents at low concentrations could influence the configuration of the ligand rather than the SBUs, thus providing an effective means of leading to conformational isomerism. This methodology is different from that described for the previously reported conformational isomers obtained by altering the solvent system from polar to nonpolar, organic to inorganic, or dry to wet and can easily achieve the conformational isomerism in a more controlled way. More importantly, we reasoned that conformational isomers **1** and **2** could be directly attributed to the anion−*π* interaction between electron-efficient atoms of templates and electron-deficient dicarboxylic acid aromatic cores in H_4pdpa introduced into the process of self-assembly.

TGA of 1−3. The TGA experiments were conducted to investigate the thermal stability of **1**−**3** (Figure S4 of the Supporting Information). The result for **1** shows a weight loss of 7.5% (calcd, 7.2%) in the range of 50−120 °C attributed to the departure of one water molecule and one methanol molecule, and **1** begins to lose its four coordinated solvent molecules at 150 °C, of which the weight is 13.4% (calcd, 13.7%). The main skeleton of **1** begins to collapse at 330 °C. The curve of **2** reveals that a preliminary weight loss of 13.9% (calcd, 14.8%) ranging from 100 to 150 °C is attributed to the removal of three water molecules and one acetonitrile molecule. After that, the decomposition of H_4pdpa ligands occurs at 330 °C. As for **3**, the weight loss of 10.0% (calcd, 10.8%) in the range of 50−200 °C is due to the departure of six lattice water molecules and two uncoordinated water molecules, and the ligands of **3** collapse at 310 °C.

Catalytic Capacity of 1−3. As useful building blocks in biochemistry and pharmacology, 2-substituted 1,4,5,6-tetrahydropyrimidine and 2-imidazoline derivatives attracted a great deal of interest for their potential anthelmintic, antidepressant, antibacterial, and fungicide activity.[23] In particular, many researchers have focused on the catalytic cascade cycloaddition reaction of aromatic nitriles with diamines because it is a direct method for synthesizing imidazoline and tetrahydropyrimidine rings according with the requirements of green chemistry.[24] However, the design and synthesis of effective heterogeneous MOF catalysts for this reaction and the relationship between the structural features of MOFs and their catalytic activities still need to be studied further.

The excellent match between the experimental and simulated PXRD patterns of **1**−**3** proved the phase purity of their bulky crystalline samples (Figure S5 of the Supporting Information). To study the potentials of **1**−**3** as heterogeneous catalysts in the catalytic cascade cycloaddition reaction of aromatic nitriles with diamines, we compared their activities with homogeneous $Co(OAc)_2$ by keeping the Co content the same (10%). Catalytic activities of **1**−**3** were initially evaluated in toluene at reflux for 4 h, with aromatic nitriles (**4a** and **4b**) and ethanediamine as substrates. As shown in Table 3, **1** and **2** were effective catalysts for the cascade cyclization of aromatic nitriles (**4a** and **4b**) with 1,2-ethanediamine, leading to **7a** and **7b**, respectively, with moderate to high yields (45−89%). In comparison, $Co(OAc)_2$ as a homogeneous catalyst gave cycloaddition products **7a** and **7b** with yields of 59 and 35%, respectively. Importantly, the catalytic activity of **2** was higher than that of **1**, giving yields of 89 and 60% for **7a** and **7b**, respectively. By contrast, **3** provided poor yields for **7a** and **7b**, indicating its catalytic capacity is lower than those of **1** and **2**. Similarly, with respect to the synthesis of 2-substituted 1,4,5,6-tetrahydropyrimidines by the cascade cycloaddition reactions of

Table 3. Catalyzed Synthesis of 2-Imidazolines from 4 with 1,2-Ethanediamine

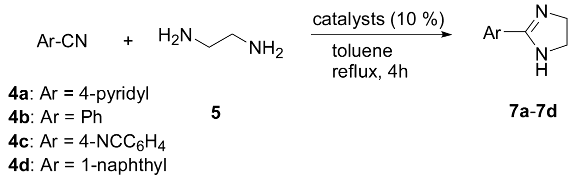

Entry	Ar	Product	Catalyst	Yield (%)
1	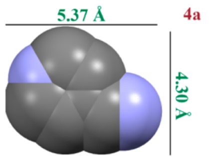	**7a**	$Co(OAc)_2$	59
2			**1**	80
3			**2**	89
4			**3**	64
5	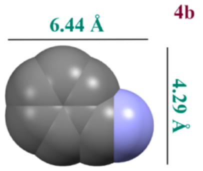	**7b**	$Co(OAc)_2$	35
6			**1**	45
7			**2**	60
8			**3**	42
9	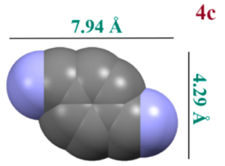	**7c**	$Co(OAc)_2$	40
10			**1**	31
11			**2**	39
12			**3**	19
13	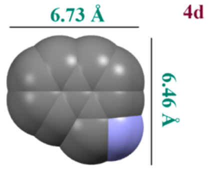	**7d**	$Co(OAc)_2$	25
14			**1**	trace
15			**2**	15
16			**3**	trace

aromatic nitriles (**4a** and **4b**) with 1,3-propanediamine, **1** gave a moderate yield, **2** was highly effective and could generate the desired products **8a** and **8b** in yields of 89 and 81%, respectively, while **3** gave poor conversions (Table 4).

Table 4. Catalyzed Synthesis of 1,4,5,6-Tetrahydropyrimidines from 4 with 1,3-Propanediamine

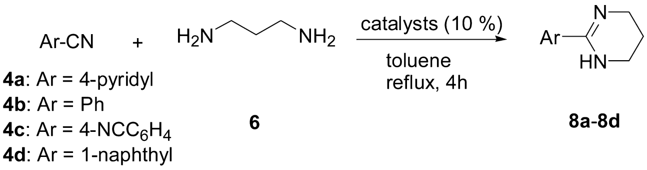

Entry	Ar	Product	Catalyst	Yield (%)
1	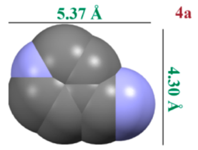	**8a**	Co(OAc)$_2$	60
2			**1**	89
3			**2**	89
4			**3**	65
5	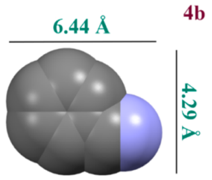	**8b**	Co(OAc)$_2$	47
6			**1**	49
7			**2**	81
8			**3**	40
9	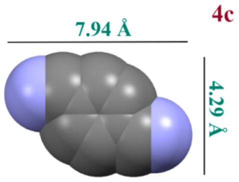	**8c**	Co(OAc)$_2$	50
10			**1**	42
11			**2**	45
12			**3**	19
13	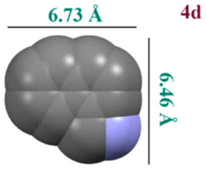	**8d**	Co(OAc)$_2$	29
14			**1**	trace
15			**2**	12
16			**3**	trace

To prove the effect of the substrate size in this reaction, we conducted the processes catalyzed by **1**−**3** with the more bulky substrates **4c** and **4d** as substrates (entries 9−16 in Tables 3 and 4). With an increase in the bulk of aromatic nitriles, the yields of reactions catalyzed by **1** and **2** obviously decreased in the order **4a** > **4b** > **4c** > **4d**, corresponding to the increase in substrate size. With the more bulky **4d**, only a trace amount of the desired compound was produced when **2** was used as a heterogeneous catalyst, while **1** and **3** were unsuitable catalysts. To eliminate the possibility of the different reactivity of **4a**−**4d** generating such a decrease, experiments were conducted with Co(OAc)$_2$ as the catalyst under the same reaction conditions. Substrates **4a**−**4d** when subjected to catalysis by Co(OAc)$_2$ did not follow the order of decrease of **1** and **2**. Therefore, the substrate size should be an important factor for determining the yield of the heterogeneous catalytic reaction.

According to the structural analysis of **1**−**3**, they exhibit various channel dimensions from ~6 Å × 6 Å for **1** to ~15 Å × 8 Å for **2** to nonporosity for **3**. The catalytic capacity of **1**−**3** increases in the order **2** > **1** > **3**, consistent with the expansion of their channel sizes. This trend indicates that the channel features could be a crucial factor in determining the reaction rate for the MOF-catalyzed cascade cycloaddition of aromatic nitriles with diamines. The pore size distributions (PSDs) of **2** after SC-CO$_2$ activation exhibit a main pore size distribution centered around 15 Å (Figure S6 of the Supporting Information). The large channels of **2** could facilitate the transport of organic substrates and products and provide enough space where substrates could access and react with catalytic active sites.[25] In addition, **1** and **2** are conformational isomers and contain the same SBUs and organic ligands but differ in the conformations of their skeletons. Conformational isomers **1** and **2** could provide an excellent platform for exploring the effect of channel size and structural features on heterogeneous catalysis because they eliminated the interference afforded by the variations of metal sites and organic ligands. As shown in entries 2 and 3 of Tables 3 and 4, both **1** and **2** are effective and give similar yields with substrate **4a**. However, with the size of the substrate increasing, the catalytic activity of **1** decreased apparently and was lower than that of **2**. For the bulky substrate **4d** with dimensions of 6.73 Å × 6.46 Å, **1** was completely inactive but **2** gave a conversion of 15% for **7d** (6.61 Å × 7.76 Å) and 12% for **8d** (6.64 Å × 8.16 Å). Because **1** and **2** have the same SBUs and elementary composition, this difference should be ascribed to the channel size of **1** not matching with bulky **4d**. As a result, **2** gave a catalytic activity higher than that of **1**, proving the importance of channel sizes to the MOF catalysts.

To further confirm that the catalytic reactions proceeded within the crystal voids, large crystals of **2** (~0.3 mm × 0.25 mm × 0.2 mm) without grinding and stirring were used as the catalyst for the synthesis of **8a**, giving a yield of 50% under the same reaction conditions. Because large crystals have too few surface catalytic sites to meet the requirement of the reaction, interior channels proved to be the place within which the reaction proceeds. Additionally, atomic absorption analysis of the filtrate showed a low level of remaining cobalt ions (<1 ppm), strongly confirming its heterogeneity.

Scheme 1. Proposed Mechanism for the Synthesis of 2-Imidazolines Catalyzed by Co-Based MOFs

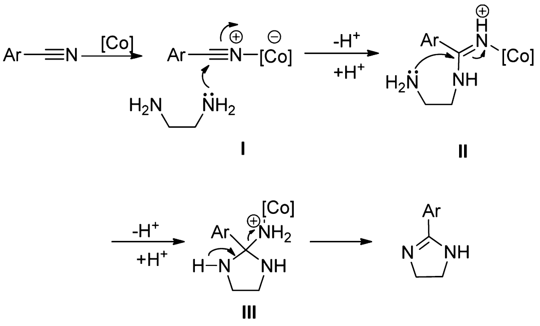

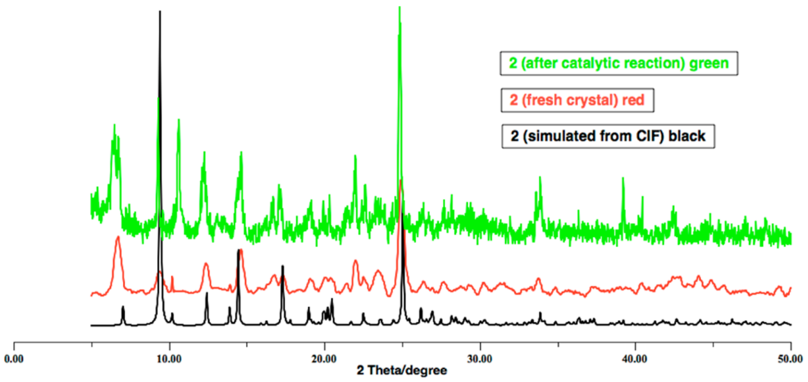

Figure 6. Comparison of the PXRD patterns of **2** before and after catalysis.

The mechanism for the synthesis of 2-imidazolines catalyzed by **2** has been proposed tentatively (Scheme 1). The nitrile is first activated by the catalyst to give **I**. Ethanediamine attacks **I** to afford **II**. Cyclization of **II** gives the final product. In addition, we reasoned that the coordination environment of metal sites in **1** and **2** also plays an important role in determining their catalytic activities. The cobalt ions in conformational isomers **1** and **2** are coordinated with not only carboxylic groups but also water molecules. Because water molecules are good leaving groups, they may facilitate departure during the catalytic process, leaving unsaturated cobalt sites exposed to aromatic nitriles.

Compared with previously reported catalysts for this kind of reaction, such as $La(OTf)_3$,[26] CuCl,[27] sulfur,[28] CS_2,[29] and H_2S,[30] **2** as a heterogeneous catalyst has several advantages, such as a higher catalytic activity stemming from its capability in stabilizing the intermediates, boosted catalyst stability arising from the spatial separation of single catalytic sites, reusability, steric hindrance selectivity, and environmental friendliness. **2** recovered from the catalytic reaction via centrifugation and filtration could be recycled and reused at least four times (Figure S7 of the Supporting Information). Moreover, the PXRD of **2** recovered from the reaction closely matched that of the pristine solid of **2**, strongly proving that **2** is stable under the catalytic condition (Figure 6).

■ CONCLUSION

In summary, with cyclic ethers (THF or 1,4-dioxane) as structure-directing agents, the assemblies of cobalt nitrate and ligand H_4pdpa under the same solvothermal condition resulted in three solvent-induced Co-based MOFs **1−3** with different structural features. Furthermore, systematically tuning the frameworks and the cavity shapes of MOFs **1−3** could be accomplished by simply changing the concentration of introduced solvent templates. The interactions between the oxygen atoms of the template guest (1,4-dioxane or THF) and electron-deficient dicarboxylic acid aromatic cores in H_4pdpa, the so-called anion−π interactions, could influence the configuration of ligand H_4pdpa and the following structural variations. In particular, in the case without solvent templates or with a low concentration of solvent templates, porous conformational isomers **1** and **2** with identical SBUs and organic ligands, but consisting of different structural skeletons and channels, were obtained. Thus, herein we provide a method for obtaining conformational isomers in a more controlled way. Further catalytic experiments showed that **2** was an effective heterogeneous catalyst for the synthesis of 2-imidazolines and 2-substituted 1,4,5,6-tetrahydropyrimidines, indicating that the channel size has a positive effect on the catalytic ability of heterogeneous catalysts.

■ ASSOCIATED CONTENT

Ⓢ Supporting Information

X-ray crystallographic information for **1−3** in CIF format, coordination environment of **1−3**, TGA plots and PXRD patterns for **1−3**, selected bond lengths and angles for **1−3**, ^{1}H NMR and ^{13}C NMR data for **7a−7d** and **8a−8d**, results of the reusability experiment, and pore size distributions of **2**. This material is available free of charge via the Internet at http://pubs.acs.org.

■ AUTHOR INFORMATION

Corresponding Authors

*E-mail: wujie@zzu.edu.cn.
*E-mail: houhongw@zzu.edu.cn. Fax: (86)371-67761744.

Notes

The authors declare no competing financial interest.

■ ACKNOWLEDGMENTS

This work was funded by the National Natural Science Foundation of China (21201152 and 21371155) and the Research Fund for the Doctoral Program of Higher Education of China (20124101110002).

■ REFERENCES

(1) (a) Hasegawa, S.; Horike, S.; Matsuda, R.; Furukawa, S.; Mochizuki, K.; Kinoshita, Y.; Kitagawa, S. *J. Am. Chem. Soc.* **2007**, *129*, 2607−2614. (b) Tanaka, K.; Oda, S.; Shiro, M. *Chem. Commun.* **2008**, 820−822. (c) Evans, O. R.; Ngo, H. L.; Lin, W. *J. Am. Chem. Soc.* **2001**, *123*, 10395−10396. (d) Henschel, A.; Gedrich, K.; Kraehnert, R.; Kaskel, S. *Chem. Commun.* **2008**, 4192−4194. (e) Horike, S.; Dinca, M.; Tamaki, K.; Long, J. R. *J. Am. Chem. Soc.* **2008**, *130*, 5854−5855. (f) Liu, J. W.; Chen, L. F.; Cui, H.; Zhang, J. Y.; Zhang, L.; Su, C. Y. *Chem. Soc. Rev.* **2014**, *43*, 6011−6061. (g) Dhakshinamoorthy, A.; Garcia, H. *Chem. Soc. Rev.* **2014**, *43*, 5750−5765.

(2) (a) Corma, A.; Garcia, H.; Llabrés i Xamena, F. X. *Chem. Rev.* **2010**, *110*, 4606−4655. (b) Tanski, J. M.; Wolczanski, P. T. *Inorg. Chem.* **2001**, *40*, 2026−2033. (c) Zhang, X.; Llabrés i Xamena, F. X.; Corma, A. *J. Catal.* **2009**, *265*, 155−160. (d) Suslick, K. S.; Bhyrappa, P.; Chou, J. H.; Kosal, M. E.; Nakagaki, S.; Smithenry, D. W.; Wilson, S. R. *Acc. Chem. Res.* **2005**, *38*, 283−291. (e) Seo, J. S.; Whang, D.; Lee, H.; Jun, S. I.; Oh, J.; Jeon, Y. J.; Kim, K. *Nature* **2000**, *404*, 982−986.

(3) (a) Corkum, E. G.; Hass, M. J.; Sullivan, A. D.; Bergens, S. H. *Org. Lett.* **2011**, *13*, 3522−3525. (b) Amarajothi, D.; Mercedes, A.; Hermenegildo, G. *ACS Catal.* **2011**, *1*, 48−53. (c) Anh, P.; Alexander,

U. C.; Felipe, G.; Carolyn, B. K.; Omar, M. Y. *Inorg. Chem.* **2011**, *50*, 7388−7390. (d) Kesanli, B.; Lin, W. B. *Coord. Chem. Rev.* **2003**, *246*, 305−326.

(4) (a) Wang, C.; Zheng, M.; Lin, W. B. *J. Phys. Chem. Lett.* **2011**, *2*, 1701−1709. (b) Ma, L.; Falkowski, J. M.; Abney, C.; Lin, W. *Nat. Chem.* **2010**, *2*, 838−846. (c) Kortunov, P. V.; Heinke, L.; Arnold, M.; Nedellec, Y.; Jones, D. J.; Caro, J.; Karger, J. *J. Am. Chem. Soc.* **2007**, *129*, 8041−8047. (d) Oxford, G. A. E.; Snurr, R. Q.; Broadbelt, L. J. *Ind. Eng. Chem. Res.* **2010**, *49*, 10965−10973. (e) Oxford, G. A. E.; Dubbeldam, D.; Broadbelt, L. J.; Snurr, R. Q. *JJ. Mol. Catal. A: Chem.* **2011**, *334*, 89−97. (f) Falkowski, J. M.; Wang, C.; Liu, S.; Lin, W. B. *Angew. Chem., Int. Ed.* **2011**, *50*, 8674−8678. (g) Huang, C.; Ding, R.; Song, C. J.; Lu, J. J.; Liu, L.; Han, X.; Wu, J.; Hou, H. W.; Fan, Y. T. *Chem.—Eur. J.* **2014**, *20*, 16156−16163.

(5) (a) Sakamoto, H.; Matsuda, R.; Bureekaew, S.; Tanaka, D.; Kitagawa, S. *Chem.—Eur. J.* **2009**, *15*, 4985−4989. (b) Li, C. P.; Zhao, X. H.; Chen, X. D.; Yu, Q.; Du, M. *Cryst. Growth Des.* **2010**, *10*, 5034−5042. (c) Li, C. P.; Yu, Q.; Chen, J.; Du, M. *Cryst. Growth Des.* **2010**, *10*, 2650−2660. (d) Yu, Q.; Zhang, X. Q.; Bian, H. D.; Liang, H.; Zhao, B.; Yan, S. P.; Liao, D. Z. *Cryst. Growth Des.* **2008**, *8*, 1140−1146. (e) Cook, T. R.; Zheng, Y. R.; Stang, P. J. *Chem. Rev.* **2013**, *113*, 734−777.

(6) (a) Chen, S. C.; Zhang, Z. H.; Huang, K. L.; Chen, Q.; He, M. Y.; Cui, A. J.; Li, C.; Liu, Q.; Du, M. *Cryst. Growth Des.* **2008**, *8*, 3437−3445. (b) Norbert, S.; Shyam, B. *Chem. Rev.* **2012**, *112*, 933−969.

(7) Huang, X. C.; Zhang, J. P.; Lin, Y. Y.; Chen, X. M. *Chem. Commun.* **2005**, 2232−2234.

(8) (a) Ma, L. Q.; Lin, W. B. *J. Am. Chem. Soc.* **2008**, *130*, 13834−13835. (b) Tynan, E.; Jensen, P.; Kruger, P. E.; Lees, A. C. *Chem. Commun.* **2004**, 776−777. (c) Schareina, T.; Schick, C.; Kempe, R. *Z. Anorg. Allg. Chem.* **2001**, *627*, 131−133.

(9) (a) Tzeng, B. C.; Yeh, H. T.; Chang, T. Y.; Lee, G. H. *Cryst. Growth Des.* **2009**, *9*, 2552−2555. (b) Senkovska, I.; Kaskel, S. *Eur. J. Inorg. Chem.* **2006**, 4564−4569. (c) Dinca, M.; Long, J. R. *J. Am. Chem. Soc.* **2005**, *127*, 9376−9377.

(10) (a) Lin, J. B.; Zhang, J. B.; Zhang, W. X.; Xue, W.; Xue, D. X.; Chen, X. M. *Inorg. Chem.* **2009**, *48*, 6652−6660. (b) Burrows, A. D.; Cassar, K.; Friend, R. M. W.; Mahon, M. F.; Rigby, S. P.; Warren, J. E. *CrystEngComm* **2005**, *7*, 548−550. (c) Li, C. P.; Du, M. *Chem. Commun.* **2011**, *47*, 5958−5972.

(11) (a) Tanaka, D.; Masaoka, S.; Horike, S.; Furukawa, S.; Mizuno, M.; Endo, K.; Kitagawa, S. *Angew. Chem., Int. Ed.* **2006**, *45*, 4628−4631. (b) Wang, D. X.; Wang, M. X. *J. Am. Chem. Soc.* **2013**, *135*, 892−897.

(12) Kasai, K.; Fujita, M. *Chem.—Eur. J.* **2007**, *13*, 3089−3105.

(13) (a) Li, C. P.; Tian, Y. L.; Guo, Y. M. *Inorg. Chem. Commun.* **2008**, *11*, 1405−1408. (b) He, M. Y.; Chen, S. C.; Zhang, Z. H.; Huang, K. L.; Yin, F. H.; Chen, Q. *Inorg. Chim. Acta* **2009**, *362*, 2569−2576. (c) Fromm, K. M.; Doimeadios, J. L. S.; Robin, A. Y. *Chem. Commun.* **2005**, 4548−4550.

(14) Li, C. P.; Du, M. *Chem. Commun.* **2011**, *47*, 5958−5972.

(15) (a) Hennigar, T. L.; MacQuarrie, D. C.; Losier, P.; Rogers, R. D.; Zaworotko, M. J. *Angew. Chem., Int. Ed.* **2003**, *36*, 972−973. (b) Zhang, K. P.; Huang, X. C.; Chen, X. M. *Chem. Soc. Rev.* **2009**, *38*, 2385−2396. (c) Makal, T. A.; Yakovenko, A. A.; Zhou, H. *J. Phys. Chem. Lett.* **2011**, *2*, 1682−1689. (d) Du, M.; Li, C. P.; Chen, M.; Ge, Z. W.; Wang, X.; Wang, L.; Liu, C. S. *J. Am. Chem. Soc.* **2014**, *136*, 10906−10909. (e) Chen, X. D.; Zhao, X. H.; Chen, M.; Du, M. *Chem.—Eur. J.* **2009**, *15*, 12974−12977.

(16) (a) Kishan, M. R.; Tian, J.; Thallapally, P. K.; Fernandez, C. A.; Dalgarno, S. J.; Warren, J. E.; McGrail, B. P.; Atwood, J. L. *Chem. Commun.* **2010**, *46*, 538−540. (b) Zhu, N. Y.; Lennox, M. J.; Duren, T.; Schmiit, W. *Chem. Commun.* **2014**, *50*, 4207−4210.

(17) (a) Chen, X. D.; Du, M.; Mak, T. C. W. *Chem. Commun.* **2005**, 4417−4419. (b) Braga, D.; Maini, L.; Mazzeo, P. P.; Ventura, B. *Chem.—Eur. J.* **2010**, *16*, 1553−1559.

(18) (a) Chen, C. Y.; Cheng, P. Y.; Wu, H. H.; Lee, H. M. *Inorg. Chem.* **2007**, *46*, 5691−5699. (b) Frahm, D.; Hoffmann, F.; Fröba, M. *Cryst. Growth Des.* **2014**, *14*, 1719−1725.

(19) Shao, X. B.; Jiang, X. K.; Wang, X. Z.; Li, Z. T.; Zhu, S. Z. *Tetrahedron* **2003**, *59*, 4881−4889.

(20) (a) Sheldrick, G. M. *SHELXS 97, Program for the solution of Crystal Structures*; University of Göttingen: Göttingen, Germany, 1997. (b) Sheldrick, G. M. *SHELXS 97, Program for the Refinement of Crystal Structures*; University of Göttingen: Göttingen, Germany, 1997.

(21) Loudon, G. M. *Organic Chemistry*, 4th ed.; Oxford University Press: New York, 2002.

(22) Fu, A. Y.; Jiang, Y. L.; Wang, Y. Y.; Gao, X. N.; Yang, G. P.; Hou, L.; Shi, Q. Z. *Inorg. Chem.* **2010**, *49*, 5495−5502.

(23) (a) Dunbar, P. G.; Durant, G. J.; Fang, Z.; Abuh, Y. F.; El-Assadi, A. A.; Ngur, D. O.; Periyasamy, S.; Hoss, W. P.; Messer, W. S. *J. Med. Chem.* **1993**, *36*, 842−847. (b) Dolinkin, A. O.; Chernov'yants, M. S. *Pharm. Chem. J.* **2010**, *44*, 99−106.

(24) An, S. J.; Yin, B.; Liu, P.; Li, X. G.; Li, C.; Li, J. L.; Shi, Z. *Synthesis* **2013**, *45*, 2525−2532.

(25) Song, F. J.; Wang, C.; Falkowski, J. M.; Ma, L. Q.; Lin, W. B. *J. Am. Chem. Soc.* **2010**, *132*, 15390−15398.

(26) Forsberg, J. H.; Spaziano, V. T.; Balasubramanian, T. M.; Liu, G. K.; Kinsley, S. A.; Duckworth, C. A.; Poteruca, J. J.; Brown, P. S.; Miller, J. L. *J. Org. Chem.* **1987**, *52*, 1017−1021.

(27) Rousselet, G.; Capdevielle, P.; Maumy, M. *Tetrahedron Lett.* **1993**, *34*, 6395−6398.

(28) Mirkhani, V.; Moghadam, M.; Tangestaninejad, S.; Kargar, H. *Teterahedron Lett.* **2006**, *47*, 2129−2132.

(29) Corbel, J. C.; Uriac, P.; Huet, J.; Martin, C. A. E.; Advenier, C. *Eur. J. Med. Chem.* **1995**, *30*, 3−13.

(30) Levesque, G.; Gressier, J.-C.; Proust, M. *Synthesis* **1981**, 963−965.